JOURNAL OF Materials CHEMISTRY

Preparation of high acicular and uniform goethite particles by a modified-carbonate route

Nuria O. Nuñez,* M. Puerto Morales, Pedro Tartaj and Carlos J. Serna

Instituto de Ciencia de Materiales de Madrid (CSIC) Campus de Cantoblanco 28049, Madrid, Spain. E-mail: nuria@icmm.csic.es

Received 22nd June 2000, Accepted 10th August 2000
First published as an Advance Article on the web 27th September 2000

A procedure for the synthesis of high acicular and uniform goethite particles based on a modified-carbonate route is reported. It essentially consists of the oxidation–precipitation of iron sulfate solutions through a two-oxidation process, which involves the formation of primary particles and their subsequent growth. XRD, TEM, colour evolution and pH monitoring have been used to determine the mechanism responsible for the formation of goethite particles with well-controlled morphology. Single-phase goethite particles are formed from initial suspensions with OH/Fe equivalent ratios from 0.05 to 0.35, which determine the supersaturation level of the solution and consequently, the length of the particles. The best conditions to prepare uniform goethite particles of 250 nm in length and high axial ratio (8), adequate as high-density audio/video media precursors, have been established.

1. Introduction

Magnetic particulate recording media consist of acicular particles deposited longitudinally on a film. Acicular particles are preferred over equiaxial ones due to the low value of the demagnetising field along the major axis. Additionally, due to the need to improve bit-packing densities, small particle sizes (above the superparamagnetic limit) and narrow size distributions are required for high density recording media.[1] Thus, magnetic particle shape and size must be optimised to account for these two effects. Nowadays, particles of about 100×20 nm of α-Fe are used in high-density audio/video tapes which result in coercivity values larger than 2000 Oe, magnetisation values of 150 emu g^{-1} and recording densities of 12 Gbytes in a tape.[2,3]

Among the different precursors that can be employed for the preparation of acicular α-Fe particles, goethite is the most frequently used.[4] The preparation of α-Fe particles essentially involves the synthesis of acicular goethite particles, their further dehydration into hematite and their reduction to iron particles.[5] Different methods have been reported for the synthesis of acicular goethite particles.[6–12] In general, particles formed by oxidation of Fe(II) solutions are usually much less developed and the crystals are smaller than those obtained in alkaline Fe(III) solutions.[12] Therefore, the aim of the present work is to describe a method based on the oxidation of Fe(II) solutions for producing small goethite particles with narrow size distributions and high axial ratios, appropriate for their use as precursors for high density recording media.

It has been reported that depending on the experimental conditions either goethite (α-FeOOH), lepidocrocite (γ-FeOOH) or magnetite (Fe_3O_4) can be obtained by oxidation of Fe^{2+} salt solutions:[11]

$$2Fe^{2+} + 3H_2O + 1/2O_2 \rightarrow 2FeOOH + 4H^+ \quad (1)$$

$$3Fe^{2+} + 3H_2O + 1/2O_2 \rightarrow Fe_3O_4 + 6H^+ \quad (2)$$

Previous investigations have also shown that goethite is preferred over the other two phases when $FeSO_4$ solution is used in the presence of carbonates.[12–14] Therefore, the method here described is based on the oxidation of iron(II) sulfate solutions in the presence of carbonates. Essentially, it consists of the preparation of goethite particles through a double-oxidation process, *i.e.* the formation of primary particles and their subsequent growth. In theory with this approach we may generate small particles with a narrow size distribution, since as previously suggested the overlap of both stages results in heterogeneous particle distributions.[15,16] The OH/Fe equivalent ratio of the initial suspensions, the reagents concentration and the nature of the base used were systematically changed to investigate their effect upon the phase composition and morphological characteristics of the final products. In addition, a detailed characterisation of the goethite particles was also carried out.

2. Experimental

2.1. Sample preparation

Analytical grade reagents (iron(II) sulfate from Fluka; sodium carbonate from Carlo Erba and sodium hydroxide from Panreac) and doubly distilled water previously deaerated with N_2, were used in all experiments.

$Fe(OH)_2$ aqueous suspensions were prepared by addition of different amounts of sodium hydroxide (OH/Fe equivalent ratio from 0.05 to 1) to a 0.1 M $FeSO_4$ solution under N_2. Immediately after, N_2 gas was replaced with air, which was bubbled through the solution at a flow rate of 5 l min^{-1} throughout. Once the pH reached a constant value ($\approx$3.5), an appropriate amount of sodium carbonate was added to the slurry to raise the pH ($1.5CO_3^{2-}$/Fe equivalents) and the oxidation was continued for a further 4 hours. The reaction was conducted at a constant temperature of 40 °C in a glass vessel and pH variations were recorded using a digital pH meter (Crison GLP21). Aliquots of samples were collected at different times from their mother solutions to follow phase evolution during the oxidation process. In some experiments the $FeSO_4$ concentration and the nature of the added base were varied to determine their effect upon the phase composition. A detailed description of the different experimental conditions is shown in Table 1.

DOI: 10.1039/b005014h

Table 1 Experimental conditions used for the goethite synthesis. Air flux = 5 l min^{-1}, T^a = 40 °C

	$[Fe^{2+}]$/M	$Base_n$	Equiv. ratio $(OH/Fe)_n$	pH_n	$Base_G$[b]	pH_G	Phase composition
1	0.1	NaOH	0.05	7.8	Na_2CO_3	9.1	Goethite
2	0.1	NaOH	0.1	7.9	Na_2CO_3	9.2	Goethite
3	0.1	NaOH	0.35	8.0	Na_2CO_3	9.7	Goethite
4	0.1	NaOH	0.5	8.1	Na_2CO_3	9.8	Goethite + Magnetite
5	0.1	NaOH	0.75	8.3	Na_2CO_3	10.3	Goethite + Magnetite
6	0.1	NaOH	1	9.7	Na_2CO_3	11.0	Magnetite
7	0.05	NaOH	0.35	8.0	Na_2CO_3	9.6	Goethite + lepidocrocite
8	0.1	NaOH	0.35	7.9	NaOH	12.4	Goethite + Magnetite

[a]Subscript n and G stand for nucleation and growth stages respectively. [b]OH/Fe equivalent ratio = 1.5.

2.2. Sample characterisation

Phase identification was carried out by X-ray diffraction (XRD) in a Philips PW1710 using Cu-Kα. XRD was also employed to determine crystallite size by using the Scherrer equation.[17] The particle size and shape of the samples was examined by transmission electron microscopy (TEM, Phillips 300). The mean size (x) and the standard deviation (SD) were evaluated from the electron micrographs by counting around one hundred particles. From these data, the degree of polydispersity, which is a way of quantifying the uniformity of a particulate solid, defined as SD/x, was calculated. Electron diffraction and HRTEM were carried out in a Jeol 2000 FX2 microscope.

3. Results and discussion

3.1. First oxidation process

The evolution of pH *versus* time during the oxidation process is shown in Fig. 1 for suspensions with a constant salt concentration (0.1 M) and different OH/Fe equivalent ratios. Three regions of almost constant pH (regions I, III and V) separated by two regions of sharp changes in pH (regions II and IV) can be observed. The fact that the length of the constant pH regions (I and III) decreases as the initial OH/Fe equivalent ratio decreases, *i.e.* smaller amount of base added, suggests that these regions must be related to the amount of $Fe(OH)_2$ in the suspensions.

The nature of the solid formed in the different regions was examined for an OH/Fe equivalent ratio of 0.35 since it results in goethite particles with the largest axial ratio. Most of the peaks observed in the X-ray diffraction pattern of solids in region I are assigned to "green rust (I)" (Fig. 2). A blue-greenish colour was developed in the suspension and TEM micrographs showed the presence of very poor crystalline materials (Fig. 3a). These observations are consistent with the mechanism previously suggested for green rust formation in the presence of SO_4^{2-} anions[18] that can be expressed by the following equation:

$$x\mathrm{Fe(OH)_3} + y\mathrm{FeSO_4}^{2-} + 2(y-z)\mathrm{OH}^- \rightarrow \mathrm{Fe}_x^{\mathrm{III}}\mathrm{Fe}_y^{\mathrm{II}}(\mathrm{OH})_{(3x+2y-2z)}(\mathrm{SO_4})_z + (y-z)\mathrm{SO_4}^{2-} \quad (3)$$

Therefore, the slow decrease in pH with time in region I in comparison with regions III and V is a consequence of the simultaneous oxidation–precipitation of part of the Fe(II) to give $Fe(OH)_3$, which would then react with the Fe(II) cations still remaining in solution to form green rust, and the release of hydroxyl anions coming from the dissolution of the $Fe(OH)_2$. Thus, the slope of the curve in this region becomes flatter as the OH/Fe equivalent ratio is increased, *i.e.* larger initial amount of $Fe(OH)_2$.

Once the green rust is formed, Fe^{2+} cations, released into the solution as a consequence of the dissolution of $Fe(OH)_2$, continue oxidising in a process that can be described by eqn. (1). Thus, a sharp decrease in pH is detected (region II) until a new region of constant pH is reached at around pH 6 (region III). This plateau most likely originates from the simultaneous occurrence of two opposite processes, *i.e.* the oxidation of Fe^{2+} and the dissolution of the green rust. In fact, the elimination of the intense green colour at the end of the region III, characteristic of the green rust, supports this interpretation. In addition, the X-ray diffraction pattern of the solids obtained from region III showed the initial formation of lepidocrocite and goethite (Fig. 2).

When the green rust has been fully dissolved, the oxidation of Fe^{2+} produces again a sharp decrease in the pH (region IV) to reach a final constant value of $\approx$3.5 (region V) (Fig. 1), which in principle could suggest the complete oxidation of Fe^{2+}. The X-ray diffractogram of the solids from region V showed the presence of two iron hydroxide phases, lepidocrocite and goethite. In agreement with this result, a TEM

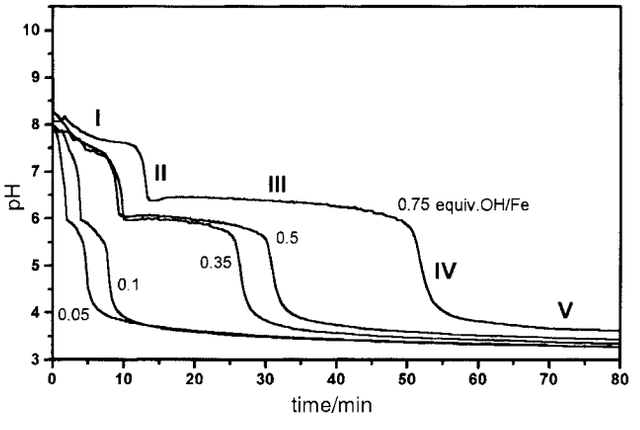

Fig. 1 Evolution of pH as a function of time and OH/Fe equivalent ratio, during the nucleation period. The experiments were carried out at 40 °C with an airflow of 5 l min^{-1} and 0.1 M $FeSO_4$.

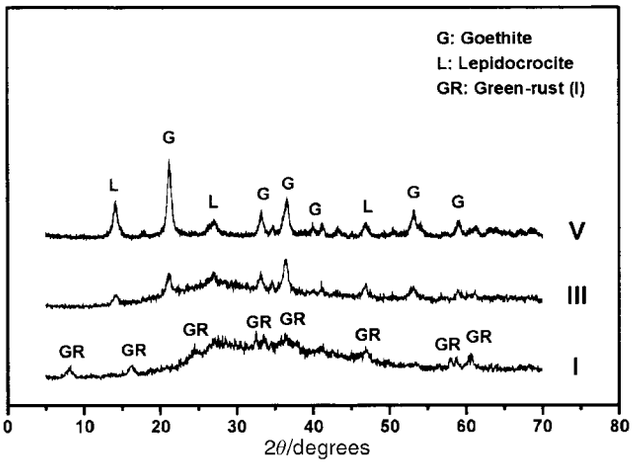

Fig. 2 X-Ray diffraction patterns for regions I, III and V of the nucleation period corresponding to the experiment with an initial OH/Fe of 0.35.

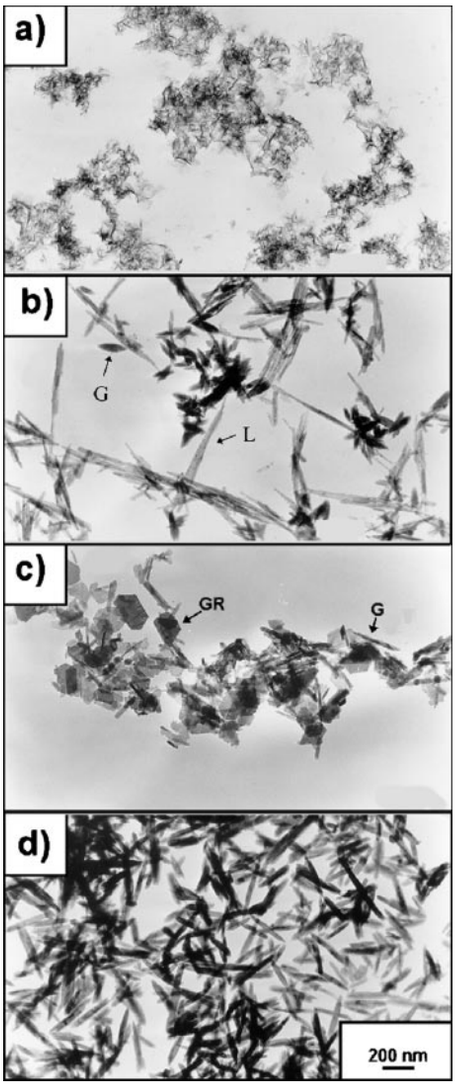

Fig. 3 TEM pictures of samples taken during the nucleation period: a) region I. b) region V and the growth period: c) initial; d) after 4 hours. The arrows marked with GR, L and G correspond to Green Rust, Lepidocrocite and Goethite, respectively.

micrograph showed the presence of large fibres corresponding to lepidocrocite along with some small elongated particles of goethite (primary particles) of about 150×30 nm (Fig. 3b). It should be noted that the proportion of goethite/lepidocrocite at the end of this stage increases as the initial OH/Fe equivalent ratio increases (data not shown).

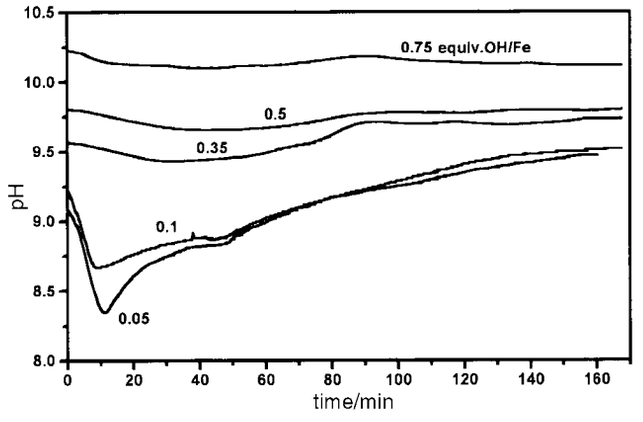

Fig. 4 Evolution of pH as a function of time and OH/Fe equivalent ratio during the growth period. The experiments were carried out at 40 °C with an airflow of 5 l min^{-1} and 0.1 M $FeSO_4$.

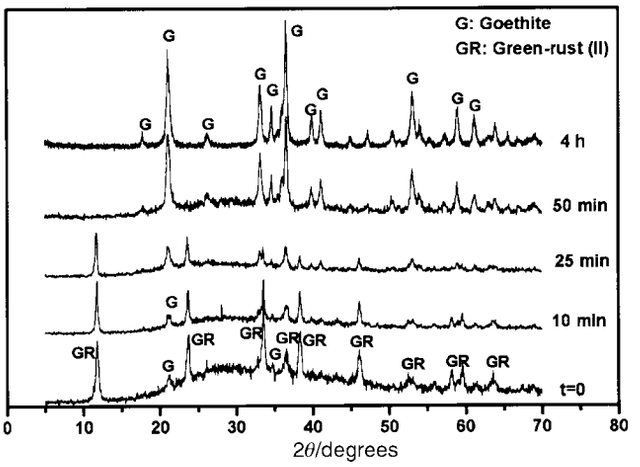

Fig. 5 X-Ray diffraction patterns of the sample with an initial OH/Fe of 0.35 during the growth period.

ICP experiments were carried out in order to determine the amount of Fe ions present in solution at the end of the first oxidation process. At this pH only Fe^{2+} cations remain in solution since all Fe^{3+} must be precipitated.[12] It was observed that even after 3 hours of oxidation, 90% of the Fe^{2+} initially added remained in solution for the sample with OH/Fe = 0.05, while the amount of Fe^{2+} ions in solution was reduced to $\approx$60% for the sample with OH/Fe = 0.35. In general, the amount of Fe^{2+} remaining in solution at this stage decreases as the OH/Fe equivalent ratio increases. It should be taken into account that the Fe^{2+} oxidation rate is mainly controlled by the amount of $Fe(OH)_2$ present in solution[19,20] which strongly decreases as the pH turns to more acidic values.[18,21] Thus, for the sample with a lower OH/Fe ratio, which reaches the region of acid pH more quickly (Fig. 1) most of the Fe^{2+} initially added is still in solution as measured by ICP.

3.2. Second oxidation process

Once goethite primary particles were formed, excess sodium carbonate was added to the slurry (CO_3/Fe equivalent ratio of 1.5), resulting in an increase in pH from 3.5 to about 9–10, depending again on the initial OH/Fe equivalent ratio (Fig. 4). Immediately after the addition, lepidocrocite is dissolved and new diffraction peaks at 10.9 and 23.7° (2θ), which are characteristic of green rust containing carbonate in its structure,[19] along with peaks corresponding to the goethite nuclei can be seen in the XRD pattern (Fig. 5). Accordingly, a green colour was again developed in the suspension. Under basic pH conditions lepidocrocite is unstable[22] and it will be dissolved releasing Fe^{3+} which forms $Fe(OH)_3$. This hydroxide reacts with the Fe^{2+} still present in solution to give green rust (II), in a similar way to that described in eqn. (3) but with carbonate instead of sulfate anions as the building blocks of the structure. A TEM micrograph of the solid obtained at the beginning of this stage is shown in Fig. 3c. Together with the laminar particles characteristic of green rust, the goethite primary particles formed at the end of the first oxidation process can be observed, which remain in suspension without undergoing any transformation since they are stable at basic pH.[21]

Apart from the slight initial decrease, the pH generally remains constant during the second oxidation process (Fig. 4) as a consequence of two different mechanisms: the dissolution of the green rust and the oxidation–precipitation of Fe^{2+}, analogous to that occurring in region (III) during the first stage (Fig. 1). According to these results, as the oxidation proceeds, diffraction peaks associated with green rust progressively disappear giving rise to the growth of the goethite primary

Table 2 Effect of the initial amount of OH^- added on final particle size and distribution for a 0.1 M $FeSO_4$ solution and a CO_3/Fe equivalent ratio of 1.5[a]

	TEM				Degree of polydispersity	
Ratio OH/Fe	*L*/nm	*w*/nm	*L*/*w*	XRD width/nm	SD/*L*	SD/*w*
0.05	150 (40)	35 (10)	4	32±5	0.27	0.28
0.1	190 (59)	35 (7)	5	37±7	0.30	0.20
0.35	240 (60)	30 (7)	8	40±12	0.25	0.23

[a]*L*: length, *w*: width, *L*/*w*: axial ratio, SD: Standard deviation.

particles (Fig. 5). The final goethite particles obtained for the sample with OH/Fe = 0.35 are shown in Fig. 3d.

For preparations with an OH/Fe equivalent ratio lower than 0.1, a sharp initial decrease in pH is observed (Fig. 4), likely due to the oxidation of the Fe^{2+} remaining in solution at the end of the first stage, which is highly concentrated. In this case, further nucleations are expected to take place at this second stage and consequently, a larger amount of goethite primary particles will be formed due to the high OH concentration (OH/Fe = 1.5). On the other hand, preparations with OH/Fe equivalent ratios higher than 0.5 give rise to the formation of magnetite together with goethite probably due to the higher pH measured at the beginning of the second stage (Table 1). It has previously been established that magnetite is the stable iron oxide phase when working at basic pH.[20,22]

The $FeSO_4$ concentration and the nature of the base added in the second oxidation process were varied to determine their effect on phase composition (Table 1). It was observed that for iron salt concentrations lower than 0.1 M a mixture of lepidocrocite and goethite was obtained. Also, when NaOH was used instead of carbonate during the second oxidation process, a mixture of magnetite and goethite was obtained, which can be related again to the strong basic pH present at the beginning of this stage (Table 1).

In conclusion, in order to obtain only goethite particles several restrictions must be considered in our system such as the use of OH/Fe ratios lower than 0.5 and iron salt concentrations higher than 0.1 M. Additionally, the presence of carbonates, at least in the second stage, seems essential to obtain pure goethite.

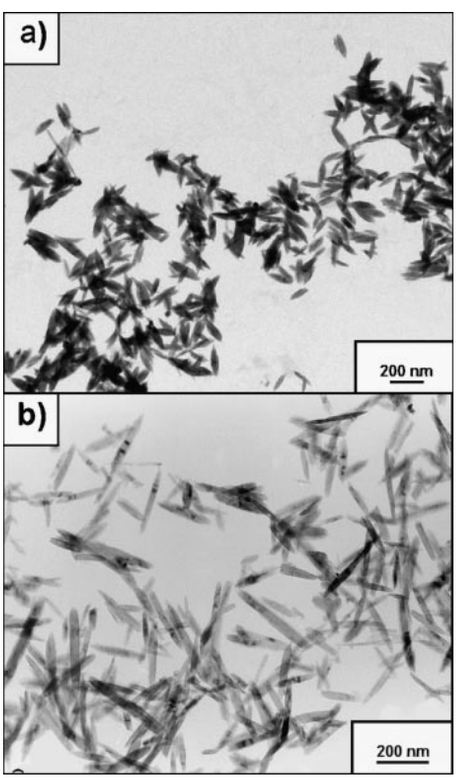

Fig. 6 TEM pictures of the goethite particles prepared with different OH/Fe equivalent ratios: a) 0.05, b) 0.35.

3.3. Morphology of goethite particles

Under the conditions described above, single-phase goethite particles are formed for OH/Fe equivalent ratios between 0.05 and 0.35. The morphological characteristics of the goethite particles are given in Table 2, together with the crystal width from the 020 X-ray reflection. The degree of polydispersity was about 25% in all cases, close to that required for the so-called uniform particles (Fig. 6). Thus, a monodispersed solid is considered when this parameter is $\leqslant 20\%$.[23] From Table 2, it can be seen that the particle length decreases (from 250 to 150 nm) as the OH/Fe equivalent ratio decreases, meanwhile the particle width remains almost constant (30–35 nm). Therefore, the goethite particles with the largest axial ratio ($L/w = 8$) are the ones obtained with an OH/Fe equivalent ratio of 0.35 (Fig. 6b). Lower OH/Fe equivalent ratios lead to the formation of smaller particles (Fig. 6a).

The mechanism of formation of pure and uniform goethite particles in the extreme cases of OH/Fe equivalent ratios 0.05 and 0.35, can be best explained on the basis of LaMer's diagram[24] (Fig. 7). It consists to a large extent in a separation of the nucleation and growth stages. For the sample prepared with OH/Fe = 0.05, most of the initial Fe^{2+} remains in solution at the end of the first oxidation process as measured by ICP. Therefore, the formation of the primary particles takes place mainly in the second stage, when carbonate is added. Since the amount of base added at this stage is much higher than in the previous one, a larger supersaturation of solute will result, giving rise to more particles of smaller size. On the contrary, for the sample with OH/Fe = 0.35, the nucleation takes place in the first stage at a lower supersaturation. The final particles are obtained by the subsequent addition of Fe^{3+} complexes, generated as a consequence of the slow dissolution of green rust onto the goethite primary particles. It should be emphasised that as the separation of the nucleation and growth

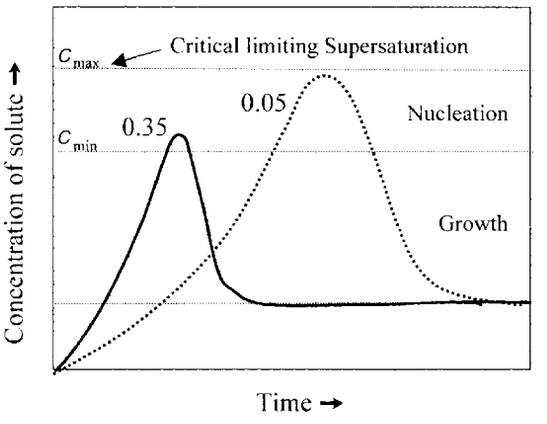

Fig. 7 Schematic diagram of the change of solute concentration with time in the case of the formation of pure uniform goethite particles with OH/Fe equivalent ratios of 0.05 and 0.35.

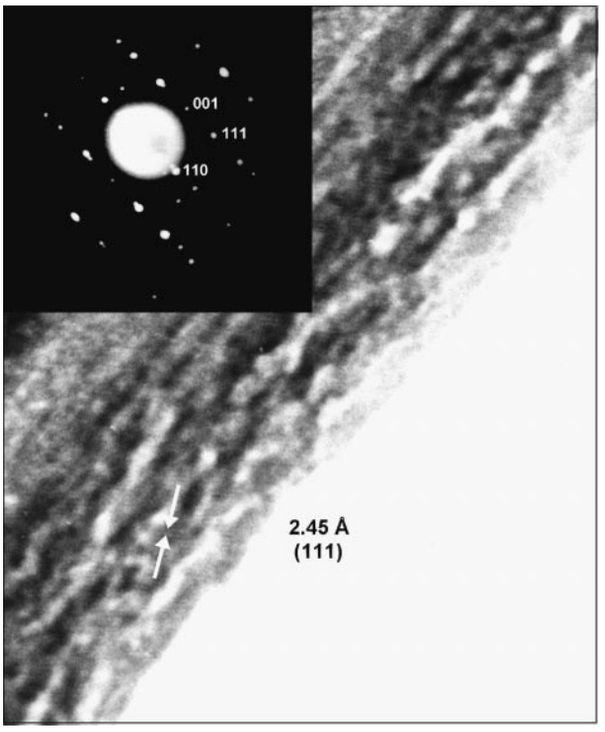

Fig. 8 HRTEM of the sample obtained with a OH/Fe equivalent ratio of 0.35. The inset shows the electron diffraction pattern from a goethite particle.

stages becomes more effective, the goethite particles become more acicular (Fig. 6b).

Crystal sizes obtained from the (020) reflection are between 30 and 40 nm (Table 2) similar to the particle width observed by TEM and suggesting that the (001) crystallographic axis is along the longest particle dimension, in accordance with the goethite crystal habit of growth.[25]

Electron diffraction carried out on a selected area of the sample with the highest axial ratio ($L/W=8$, Fig. 8) gives clear diffraction spots characteristic of goethite, which have been assigned to the planes (001), (111) and (110). Therefore, the particles have monocrystalline character in agreement with X-ray data. Fig. 8 also shows a high-resolution electron micrograph, which illustrates the particle texture along the planes (111).

4. Conclusions

Uniform acicular goethite particles can be prepared by the oxidation–precipitation of $FeSO_4$ in the presence of NaOH and Na_2CO_3 through a two-oxidation process, which attempts to separate the nucleation and growth stages. It has been observed that for 0.1 M $FeSO_4$ concentrations, pure goethite particles with different particle length are obtained by using OH/Fe equivalent ratio values from 0.05 to 0.35 at the first stage and 0.15 M Na_2CO_3 at the second stage. Finally, goethite particles with an axial ratio up to 8 and a length smaller than 250 nm are obtained for a OH/Fe equivalent ratio of 0.35.

Acknowledgements

This work was supported by the CICYT under project PB98-0525. N. O. Nuñez gratefully acknowledges her fellowship from the Agencia Española de Cooperación Iberoamericana.

References

1 K. O'Grady and H. Laidler, *J. Magn. Magn. Mater.*, 1999, **200**, 616.
2 S. Hisano and K. Saito, *J. Magn. Magn. Mater.*, 1998, **190**, 371.
3 M. P. Morales, S. A. Walton, L. S. Prichard, C. J. Serna, D. P. E. Dickson and K. O'Grady, *J. Magn. Magn. Mater.*, 1998, **190**, 357.
4 K. Tagawa, K. Sudoh, S. Takahashi, M. Matsunaga and K. Ohshima, *IEEE Trans. Magn.*, 1985, **21**, 1492.
5 M. P. Sharrock and R. E. Bodnar, *J. Appl. Phys.*, 1985, **57**, 3919.
6 U. Schwertmann, P. Cambier and E. Murad, *Clays Clay Miner.*, 1985, **33**, 369.
7 R. G. Ford, P. M. Bertsch and J. C. Seaman, *Clays Clay Miner.*, 1997, **45**, 769.
8 R. M. Cornell and R. Giovanoli, *Clays Clay Miner.*, 1985, **33**, 424.
9 L. Pérez-Maqueda, J. M. Criado, C. Real, J. Šubrt and J. Bohácek, *J. Mater. Chem.*, 1999, **9**, 1839.
10 R. M. Cornell, A. M. Posner and J. P. Quirk, *J. Inorg. Nucl. Chem.*, 1974, **36**, 1937.
11 C. Domingo, R. Rodríguez-Clemente and M. A. Blesa, *Colloids Surf. A.*, 1993, **79**, 177.
12 (*a*) R. M. Cornell and U. Schwertmann, *The Iron Oxides. Structure, Properties, Reactions, Occurrence and Uses*, VCH, Weinheim, Germany, 1996, pp. 63; (*b*) R. M. Cornell and U. Schwertmann, *The Iron Oxides. Structure, Properties, Reactions, Occurrence and Uses*, VCH, Weinheim, Germany, 1996, pp. 344–345.
13 T. Atsushi, K. Hiroyuki, I. Masaru, Y. Yoshitaka, H. Tosiharu, O. Yosiro, S. Hiroshi, K. Hirofumi and M. Kohji, Toda Kogyo Corp., Japan Patent JP 87011/84, 1984.
14 Y. Katsumi, H. Kurokawa, H. Tosiharu, I. Kazuhiza, S. Hideaki, M. Tomohisa and K. Junichi, Toda Kogyo Corp., Japan Patent JP 157831/91, 1991.
15 E. Sada, H. Kumazawa, K. Makino and H. M. Cho, *Chem. Eng. Commun.*, 1990, **91**, 225.
16 E. Matijevic, *Chem. Mater.*, 1993, **5**, 412.
17 L. V. Azároff, *Elements of X-ray Crystallography*, McGraw-Hill, New York, USA, 1968, pp. 549–552.
18 C. Domingo, R. Rodríguez-Clemente and M. A. Blesa, *Solid State Ionics*, 1993, **59**, 187.
19 S. H. Drissi, Ph. Refait, M. Abdelmoula and J. M. R. Génin, *Corros. Sci.*, 1995, **37**, 2025.
20 T. Sugimoto and E. Matijevic, *J. Colloid Interface Sci.*, 1980, **74**, 227.
21 T. Misawa, K. Hashimoto and S. Shimodaira, *Corros. Sci.*, 1974, **14**, 131.
22 C. Domingo, R. Rodríguez-Clemente and M. A. Blesa, *Mater. Res. Bull.*, 1991, **26**, 47.
23 R. Hunter, *Foundations of Colloid Science*, Clarendon Press, Oxford, UK, 1987, p. 127.
24 V. K. LaMer and R. J. Dinegar, *J. Am. Chem. Soc.*, 1950, **72**, 4847.
25 M. Cornell, S. Mann and J. Skarnulis, *J. Chem. Soc., Faraday Trans. 1*, 1983, **79**, 2679.